ResearchGate

See discussions, stats, and author profiles for this publication at: https://www.researchgate.net/publication/225058713

Quantum chemical insights into the aggregation induced emission phenomena: A QM/MM study for pyrazine derivatives

ARTICLE *in* JOURNAL OF COMPUTATIONAL CHEMISTRY · SEPTEMBER 2012

Impact Factor: 3.59 · DOI: 10.1002/jcc.23019 · Source: PubMed

CITATIONS
23

READS
78

5 AUTHORS, INCLUDING:

Qunyan Wu
Tsinghua University
15 PUBLICATIONS **125** CITATIONS
SEE PROFILE

Qian Peng
Chinese Academy of Sciences
66 PUBLICATIONS **1,417** CITATIONS
SEE PROFILE

Yingli Niu
National Center for Nanoscience and Techno…
45 PUBLICATIONS **506** CITATIONS
SEE PROFILE

Zhigang Shuai
Tsinghua University
319 PUBLICATIONS **10,077** CITATIONS
SEE PROFILE

Available from: Qunyan Wu
Retrieved on: 25 January 2016

Quantum Chemical Insights into the Aggregation Induced Emission Phenomena: A QM/MM Study for Pyrazine Derivatives

Qunyan Wu,[a] Chunmei Deng,[b] Qian Peng,[b] Yingli Niu,[b] and Zhigang Shuai*[a,b]

There have been intensive studies on the newly discovered phenomena called aggregation induced emission (AIE), in contrast to the conventional aggregation quenching. Through combined quantum mechanics and molecular mechanics computations, we have investigated the aggregation effects on the excited state decays, both via radiative and nonradiative routes, for pyrazine derivatives 2,3-dicyano-5,6-diphenylpyrazine (**DCDPP**) and 2,3-dicyanopyrazino phenanthrene (**DCPP**) in condensed phase. We show that for **DCDPP** there appear AIE for all the temperature, because the phenyl ring torsional motions in gas phase can efficiently dissipate the electronic excited state energy, and get hindered in aggregate; while for its "locked"-phenyl counterpart, **DCPP**, theoretical calculation can only give the normal aggregation quenching. These first-principles based findings are consistent with recent experiment. The primary origin of the exotic AIE phenomena is due to the nonradiative decay effects. This is the first time that AIE is understood based on theoretical chemistry calculations for aggregates, which helps to resolve the present disputes over the mechanism. © 2012 Wiley Periodicals, Inc.

DOI: 10.1002/jcc.23019

Introduction

The development of efficient organic light-emitting diodes has attracted much attention because of its applications in display and lighting.[1] Highly efficient emission from organic materials is often hindered by the concentration quenching of the luminescence in the solid state, due to electron transfer, energy transfer, or Davydov splitting, which could be a thorny obstacle to the application of efficient light-emitting devices.[2] However, recently, a series of luminogens have been found to demonstrate aggregation enhanced light emitting, namely, their aggregate and/or solid states manifest much stronger light emission than in dilute solutions, in sharp contrast to the traditional aggregation quenching.[3–11] This is now termed in literature as aggregation induced emission (AIE) phenomena.[3,4] Several mechanisms have been proposed which need to be clarified, including intramolecular rotation,[7] J-aggregate formation,[8] excimer,[9] intramolecular planarization,[10] or intramolecular charge transfer.[11]

It is intriguing to understand the mechanism of such unusual phenomenon. From quantum chemical calculation, Yin *et al*. found that in silole, a group of five-member silacycles, the low-frequency phenyl ring twisting motions tend to strongly dissipate the electronic excited state energy.[12] It was shown that isopropyl substitution at proper sites cause severe hindrance to the phenyl ring twisting which eventually block the nonradiative decay channel as evidenced from the first-principles calculation of nonradiative decay rates. This provided a preliminary understanding of AIE from quantum chemistry. Peng *et al*. further pointed out that the molecular vibration modes with low-frequency tend to mix each other upon photoexcitation, and such mixing known as Duschinsky rotation effect (DRE) can strongly enhance the nonradiative energy dissipation process due to the spreadout of Franck–Condon (FC) factors.[13] The AIE phenomena was understood from the calculations of nonradiative decay processes as a function of temperature in tetraphenylbutadienes: lowering the temperature resembles to some extent the aggregate effect. Upon increasing temperature, the vibration quanta are becoming larger, and low frequency modes are getting coupled to each other through DRE, which greatly increases the nonradiative decay.[13] Our most recent calculations on the radiative and nonradiative decay processes in pyrazine derivatives also confirmed such trends, namely, for compounds with floppy phenyl rings, the temperature dependence of radiationless decay is much more pronounced than in the rigid compound.[14]

These previous theoretical studies have provided some limited insights into AIE phenomena at molecular level, namely, the importance of low-frequency side-chain motions coupled with main chain electronic excitation. But as to which extent

[a] *Q. Wu, Z. Shuai*
Department of Chemistry, MOE Key Laboratory of Organic OptoElectronics and Molecular Engineering, Tsinghua University, Beijing 100084, People's Republic of China
E-mail: zgshuai@tsinghua.edu.cn

[b] *C. Deng, Q. Peng, Y. Niu, Z. Shuai*
Key Laboratory of Organic Solids, Beijing National Laboratory for Molecular Science (BNLMS), Institute of Chemistry, Chinese Academy of Sciences, Beijing 100190, People's Republic of China

Contract/grant sponsors: China Postdoctoral Science Foundation and National Natural Science Foundation of China; contract/grant numbers: 90921007, 20903102, and 21103097 Contract/grant sponsor: Ministry of Science and Technology of China (973 program); contract grant number: 2009CB623600

© 2012 Wiley Periodicals, Inc.

these motions could be eventually influenced at solid state, which is primarily the purpose of this study. Very recently, Hayashi and coworkers investigated the nonradiative decay process of diphenyldibenzofulvene in solid phase with the ONIOM method.[15] Here, we use a quantum mechanics and molecular mechanics (QM/MM) approach coupled with a more elaborated formalism for treating nonradiative decay of molecular excited state. To study explicitly, the molecular aggregate influences on both the radiative and nonradiative decays, taking two pyrazine derivatives as examples. 2,3-dicyano-5,6-diphenylpyrazine (**DCDPP**) was found to demonstrate AIE phenomena and 2,3-dicyanopyrazino phenanthrene (**DCPP**), where the two phenyl rings in **DCDPP** are linked by a chemical bond, which demonstrate normal aggregation quenching (Scheme 1).[6] Although radiationless transitions in pyrazine has been thoroughly investigated, both experimentally and

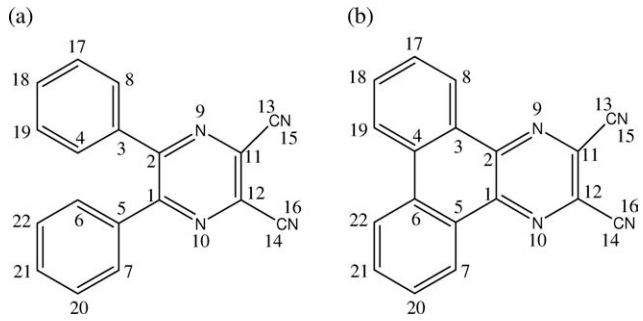

Scheme 1. The structure of the **DCDPP** molecule (a), and **DCPP** molecule (b).

theoretically.[16] Two pyrazine derivatives **DCDPP** and **DCPP** were only investigated by experiment and theory recently.[6,14] Experimentally, **DCDPP** when solved in tetrahydrofuran solution is almost nonemissive with a fluorescence quantum yield about 0.015%. However, when large amount of water is added into the solution, **DCDPP** molecules start to aggregate due to the polarity mismatch and the fluorescence yield is increased 25 times.[6] But for **DCPP**, it exhibits strong emission in solution and a normal aggregation quenching was found. As these two molecules are so similar in structure but exhibit such sharp contrast photophysical behaviors, we apply the quantum chemical method to quantitatively study their photophysical properties to gain deeper insights into the AIE phenomena.

Methodology

The molecular light-emitting efficiency is determined by the competition between the radiative decay rate (k_r) and the nonradiative decay rate (k_{nr}) from the electronically excited state to the ground state. The fluorescence quantum yield can be expressed as following: $\eta_f = k_r/(k_r + k_{nr})$. Therefore, it is essential to either suppress the nonradiative process or to increase the radiative process to attain highly efficient fluorescence. The k_{nr} is generally the sum of the internal conversion (IC) rate (k_{ic}) and the intersystem crossing rate (k_{isc}). Generally speaking, the spin-orbital coupling is very small for $\pi \rightarrow \pi^*$ electron transition, the Highest Occupied Molecular Orbital (HOMO) and Lowest Unoccupied Molecular Orbital (LUMO) for both **DCDPP** and **DCPP** describe the π and anti-π molecular orbital, respectively.[14] So, we did not consider the intersystem crossing process for **DCDPP** and **DCPP** cluster. The excited state dynamics is a formidable challenge to theoretical chemistry. There have been progresses in treating the conical intersections (CIs) and photoinduced electron dynamics,[17] for example, by the Ehrenfest dynamics,[18] surface hopping dynamics,[19] or the multiconfigurational time-dependent Hartree algorithm,[20] which has been successfully applied to treat the nonadiabatic electron dynamics for molecular photo dissociation and photo-excitation phenomena.[21] However, the quantum excited state nonadiabatic dynamics describes typically subpicosecond process ($<10^{-12}$ s), far shorter than the excited state processes in organic light-emitting materials, which is typically at time scale of $\sim 10^{-7}$–10^{-8} s. Furthermore, the light emitting device works in solid state, therefore, the photochemical reaction or CI should not be the dominant process. Otherwise, the device would degrade immediately, which is not the case. For complex polyatomic molecule, the degrees of freedom of nuclear motions are usually large, and each of them could be reasonably assumed to move not far away from the equilibrium upon photo- and electro-excitation. Thus, our choice to describe the excited state process is based on rate formalism. We adopt a multidimensional mixed harmonic oscillator model to describe the nonadiabatic processes.[22] The displaced harmonic oscillator approximation model was first outlined by Robinson and Frosch.[23] Then, the concepts and theory of radiationless transition in isolated molecules were first formulated.[24] Displaced harmonic oscillators model have been considered for small polyatomic molecules with limited DRE mode mixing by Lin and coworkers.[22]

Radiative decay rate

The radiative decay rate can be computed by the Einstein spontaneous emission which eventually can be expressed by the integration over the whole emission spectrum:

$$k_r(T) = \int \sigma_{em}(\omega, T) d\omega \quad (1)$$

where,

$$\sigma_{em}(\omega, T) = \frac{4\omega^3}{3\hbar c^3} \sum_{v_i, v_f} P_{iv_i}(T) \left| \langle \Theta_{fv_f} | \vec{\mu}_{fi} | \Theta_{ivi} \rangle \right|^2 \delta(\omega_{iv_i fv_f} - \omega) \quad (2)$$

P_{iv_i} is the Boltzmann distribution function for the initial state vibronic manifold. Θ is the vibrational wavefunction, and v_f and v_i are vibrational quantum numbers. $\vec{\mu}_{fi} = \langle \Phi_f | \vec{\mu} | \Phi_i \rangle$ is the electric transition dipole moment between two electronic states $|\Phi_i\rangle$ and $|\Phi_f\rangle$, and can be expanded in the normal coordinates as:

$$\vec{\mu}_{fi} = \vec{\mu}_0 + \sum_k \vec{\mu}_k Q_k + \sum_{k,l} \vec{\mu}_{kl} Q_k Q_l + \cdots \quad (3)$$

$\vec{\mu}_k$ and $\vec{\mu}_{kl}$ are the first and second derivatives of the electric transition dipole moment, respectively. Considering the strongly allowed transitions of the molecules in this article, the

zeroth-order term $\vec{\mu}_0$ (FC approximation) is only taken into account. Applying the Fourier transformation to the delta function in the eq. (2), we can obtain an analytical integral formalism:

$$\sigma_{em}^{FC}(\omega) = \frac{2\omega^3}{3\pi\hbar c^3}|\vec{\mu}_0|^2 \int_{-\infty}^{\infty} e^{-i(\omega-\omega_{if})t} Z_{iv}^{-1} \rho_{em,0}^{FC}(t,T)dt \quad (4)$$

Here, Z_{iv} is the partition function, and $\rho_{em,0}^{FC}(t,T) = = Tr[e^{-i\tau_f \widehat{H_f}} e^{-i\tau_i \widehat{H_i}}]$. where, $\tau_i = -i\beta - t/\hbar$, $\tau_f = t/\hbar$, and $\beta = (k_B T)^{-1}$, k_B is the Boltzmann constant. $\hat{H}_f$ and $\hat{H}_i$ is the final and initial electronic state hamiltonian of multidimensional harmonic oscillators, with which eq. (4) can be solved analytically by virtue of Gaussian integration in the path integral framework:

$$\rho_{em,0}^{FC}(t,T) = \sqrt{\frac{\det[a_f a_i]}{\det[K]}} \exp\left\{-\frac{i}{\hbar}\left[\frac{1}{2}\underline{F}^T K \underline{F} - \underline{D}^T E \underline{D}\right]\right\} \quad (5)$$

where a_i and a_f are diagonal matrices, with diagonal elements $a_k(\tau) = \omega_k/\tan(\hbar\omega_k\tau)$ and $b_k(\tau) = \omega_k/\tan(\hbar\omega_k\tau)$, respectively. $\underline{D}$ is a displacement vector connecting the minima of the parabolas of the two electronic states. $E = b_i - a_i$, $\underline{F} = \left[\underline{D}^T ES \quad \underline{D}^T ES\right]^T_{1\times 2N'}$ $K = \begin{bmatrix} B & -A \\ -A & B \end{bmatrix}_{2N\times 2N}$, here, A and B are: $A = a_f + S^T a_i S$ and $B = b_f + S^T b_i S$. Much more details of mathematical forms are listed in our previous work.[25]

IC rate

According to Fermi's golden rule, the nonradiative IC rate can be expressed as

$$k_{ic} = \frac{2\pi}{\hbar}\left|H'_{fi}\right|^2 \delta(E_{fi} + E_{fv_f} - E_{iv_i}) \quad (6)$$

Here, the perturbation is the non-Born–Oppenheimer coupling:

$$H'_{fi} = -\hbar^2 \sum_l \left\langle \Phi_f \Theta_{fv_f} \left| \frac{\partial \Phi_i}{\partial Q_{fl}} \frac{\partial \Theta_{iv_i}}{\partial Q_{fl}} \right\rangle \right. \quad (7)$$

Applying the Condon approximation, eq. (7) becomes

$$H'_{fi} = \sum_l \langle \Phi_f | \hat{P}_{fl} | \Phi_i \rangle \left\langle \Theta_{fv_f} \left| \hat{P}_{fl} \right| \Theta_{iv_i} \right\rangle \quad (8)$$

where $\hat{P}_{fl} = -i\hbar \frac{\partial}{\partial Q_{fl}}$ is the normal momentum operator.

Inserting eq. (8) into eq. (6), the IC rate can be expressed as

$$k_{IC} = \sum_{kl} k_{ic,kl} \quad (9)$$

where,

$$k_{ic,kl} = \frac{2\pi}{\hbar} R_{kl} Z_{iv}^{-1} \sum_{v_i, v_f} e^{-\beta E_{iv_i}} P_{kl} \delta(E_{fi} + E_{fv_f} - E_{iv_i}) \quad (10)$$

and

$$R_{kl} = \langle \Phi_f | \hat{P}_{fk} | \Phi_i \rangle \langle \Phi_i | \hat{P}_{fl} | \Phi_f \rangle \quad (11)$$

$$P_{kl} = \left\langle \Theta_{fv_f} \left| \hat{P}_{fk} \right| \Theta_{iv_i} \right\rangle \langle \Theta_{iv_i} | \hat{P}_{fl} | \Theta_{fv_f} \rangle \quad (12)$$

The delta function is Fourier transformed as

$$k_{ic,kl} = \frac{1}{\hbar^2} R_{kl} \int_{-\infty}^{\infty} dt \left[e^{i\omega_{if}t} Z_{iv}^{-1} \rho_{ic,kl}(t,T)\right] \quad (13)$$

where $\rho_{ic,kl}(t,T)$ is the thermal vibrational correlation function in the IC process,

$$\rho_{ic,kl}(t,T) = Tr\left(\hat{P}_{fk} e^{-i\tau_f \hat{H}_f} \hat{P}_{fl} e^{-i\tau_i \hat{H}_i}\right) \quad (14)$$

The final form of the IC correlation function is

$$\rho_{ic,kl}(t,T) = \sqrt{\frac{\det[a_f a_i]}{\det[K]}} \exp\left\{-\frac{i}{\hbar}\left[\frac{1}{2}\underline{F}^T K^{-1} \underline{F} - \underline{D}^T E \underline{D}\right]\right\} \times \left\{i\hbar Tr\left[G_{kl} K^{-1}\right] + \left(K^{-1}\underline{F}\right)^T G_{kl} \left(K^{-1}\underline{F}\right) - (H_{kl})^T K^{-1} \underline{F}\right\} \quad (15)$$

Similar to the thermal vibration correlation function eq. (5), in IC correlation function eq. (15), a_i, a_f, and E are still ($N \times N$) matrices, K is ($2N \times 2N$) matrix, $\underline{D}$ is ($N \times 1$) matrices, $\underline{F}$ is ($2N \times 1$) matrices, G_{kl} and H_{kl} are the ($2N \times 2N$) and ($1 \times 2N$) matrices, respectively. The more details of IC correlation function are given in Ref. [25]. The advantages of our correlation function formalism lie in that (i) it is fully analytical and (ii) the vibration modes mixing effect has been fully taken into account[26] which was shown to be essential for low frequency motions since these modes become mixed when electronic state is excited, expressed as $Q_k^e = \sum S_{kj} Q_j^g + D_k$, where S_{kj} is the Duschinsky rotation matrix and the vector D_k is the rigid shift in potential energy surface minimum[12,25–27]; (iii) all the vibration modes are taken into accounts when evaluating the nonadiabatic transition moment R_{kl}, including both diagonal and nondiagonal, instead of selecting only one specific mode called 'promoting mode' in previous theory.[27] Such formalism has been shown to be reasonable in describing the photophysical properties for organic polyatomic systems when CI is not involved: the decay of rate of CI is usually greater than 10^{12} s^{-1}. Namely, our formalism is applicable both for radiative and nonradiative decay rate less than 10^{12} s^{-1}. Otherwise, the rate assumption should be cautioned. The quantities required in this formalism can be obtained by DFT/Time-Dependent Density Functional Theory (TDDFT), including the vertical and adiabatic molecular excited state energies, the harmonic vibrational mode frequencies for the QM region including the MM environment and the displacement vectors between the excited state and the ground state. Reimers' algorithm is applied to calculate the Duschinsky rotation matrix and the displacement vector.[28]

Computational Details

QM/MM has been extensively used for dealing with numerous complex systems in chemical phenomena.[29] It treats a

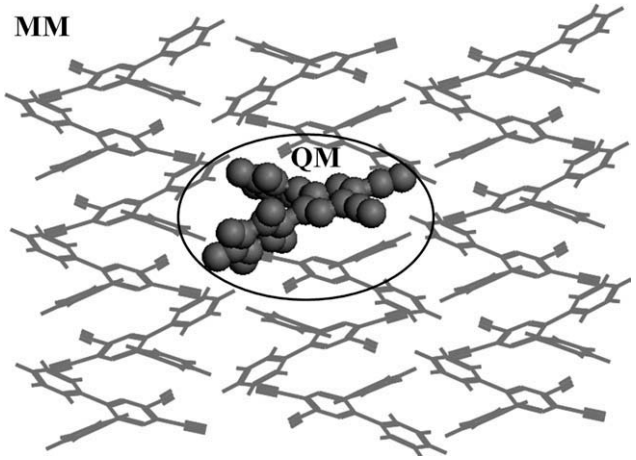

Figure 1. The set up of the QM/MM for the cluster with 18 molecules from the crystal structure (**DCDPP** as example).

relatively small localized region of the system at a high level of theory (QM) where the key chemical process takes place, whereas the remainder of the system can be adequately calculated using computationally efficient lower level methods (MM). AIE effects could be modeled by a quantum chemical calculation that takes the aggregation into account by a force field. Our setup of computational model for **DCDPP** is shown in Figure 1, where a cluster of 18 molecules are cut from the X-ray diffraction crystal structure,[6] consisting of 32 QM atoms and 544 MM atoms. We also depict the intermolecular distances in Supporting Information Figure S1. The QM/MM calculations were performed with the ChemShell interface package,[30] which perform the geometry optimization through the HDLC optimizer.[31] Turbomole 6.0[32] and DL-POLY program package[33] were used to calculate the energies and gradients of the QM and MM region, respectively. All QM calculations were performed using density functional theory (DFT) with the B3LYP functional and the 6-31G(d) basis set and the TDDFT method was applied to optimize the first excited electronic state geometries. The MM part is treated by with the General Amber force field.[34] The electrostatic embedding scheme was applied in the QM/MM calculations,[35] namely, the interaction between QM region and the MM surroundings are only through electrostatic potential.

In our QM/MM optimization, we consider only the electrostatic contribution. Thus, the fluctuation arising from the treatment of QM–MM boundary is automatically turned off. The so-called active region is only the QM part, namely, only one molecule. In this way, the variation with respect to the size of the surroundings is quite smooth. We have predicted the results for 12 and 34-molecule clusters. The numerical calculations of 34-molecule clusters did not show appreciable fluctuations on both the excitation energy as well as the geometry optimization for the phenyl ring twisting angles, while the calculations of 12-molecule clusters did. For the sake of save the computational cost, the present cluster with 18 molecules was optimized with QM/MM method. The computational model of **DCPP** is shown in Supporting Information Figure S2. We assume that the intermolecular interaction is weak that there does not occur any appreciable charge transfer or energy transfer between molecules. The intermolecular electrostatic interaction can influence the ground state and the excited state electronic structure as well as the vibronic couplings for the QM region.

The harmonic vibrational frequencies for the ground and the excited states were calculated by finite differencing of the gradients at their equilibrium geometries with ChemShell program. The transition electric field of the electronic coupling factor for the IC rate is calculated at the TDDFT level using Gaussian 09 program.[36] Based on the electronic structure information of the QM part, the Duschinsky rotation matrix and the normal mode displacements between the two electronic states, as well as the radiative and nonradiative decay rates with DRE were calculated.

Results and Discussion

We present the calculated k_r and k_{nr} with DRE for **DCDPP** molecule in cluster in Table 1 and for **DCPP** molecule in cluster in Table 2 in a wide range of temperature. We found that:

1. in all the cases, the radiative decay rate k_r are insensitive to temperature, because even though the emission spectrum

Table 1. The calculated radiative transition rate (k_r) and nonradiative transition rate (k_{nr}) with DRE from $\mathbf{S_1}$ to $\mathbf{S_0}$ and the fluorescence quantum yield (η_f) for the **DCDPP** cluster.

	Cluster			Isolated molecule[a]		
T (K)	k_r (s^{-1})	k_{nr} (s^{-1})	η_f	k_r (s^{-1})	k_{nr} (s^{-1})	η_f
300	7.55×10^6	1.78×10^7	0.30	9.32×10^6	4.45×10^9	0.21×10^{-2}
250	7.95×10^6	8.96×10^6	0.47	9.83×10^6	2.44×10^9	0.40×10^{-2}
200	8.34×10^6	4.50×10^6	0.65	1.04×10^7	1.21×10^9	0.85×10^{-2}
150	8.70×10^6	2.36×10^6	0.78	1.09×10^7	5.32×10^8	0.02
100	9.03×10^6	1.37×10^6	0.87	1.14×10^7	2.14×10^8	0.05
77	9.15×10^6	1.12×10^6	0.89	1.16×10^7	1.40×10^8	0.08
50	9.26×10^6	9.58×10^5	0.91	1.18×10^7	9.01×10^7	0.12
20	9.30×10^6	9.04×10^5	0.91	1.20×10^7	6.75×10^7	0.15

[a] Ref. [14].

Table 2. The calculated radiative transition rate (k_r) and nonradiative transition rate (k_{nr}) with DRE from $\mathbf{S_1}$ to $\mathbf{S_0}$ and the fluorescence quantum yield (η_f) for the **DCPP** cluster.

	Cluster			Isolated molecule[a]		
T (K)	k_r (s^{-1})	k_{nr} (s^{-1})	η_f	k_r (s^{-1})	k_{nr} (s^{-1})	η_f
300	1.64×10^6	8.37×10^5	0.66	1.59×10^6	3.29×10^5	0.83
250	1.71×10^6	5.12×10^5	0.77	1.60×10^6	2.74×10^5	0.85
200	1.78×10^6	3.30×10^5	0.84	1.61×10^6	2.42×10^5	0.87
150	1.85×10^6	2.26×10^5	0.89	1.61×10^6	2.25×10^5	0.88
100	1.90×10^6	1.68×10^5	0.92	1.62×10^6	2.15×10^5	0.88
77	1.93×10^6	1.52×10^5	0.93	1.62×10^6	2.13×10^5	0.88
50	1.94×10^6	1.40×10^5	0.93	1.62×10^6	2.11×10^5	0.88
20	1.95×10^6	1.36×10^5	0.93	1.62×10^6	2.09×10^5	0.89

[a] Ref. [14].

is broadened by increasing temperature, however, the radiative rate is proportional to the integration area over the whole spectrum, which become almost independent of temperature,

2. the molecular aggregate has much less effect on the radiative decay rate k_r. In this work, we did not consider the excitonic effects.[37] In fact, in many of the AIE system, both the absorption and emission spectra do not shift appreciably from solution to solid state, namely, the excitonic effect might be prominent for well-ordered single crystal but might not be the dominant effect for the thin film,

3. aggregate strongly influences the nonradiative decay in **DCDPP**. For instance, at 300 K, k_{nr} decreases from 4.45×10^9 s^{-1} in gas phase to 1.78×10^7 s^{-1} in aggregate. But in sharp contrast, for **DCPP**, aggregate only slightly increases k_{nr} from single molecule to molecule-in-cluster,

4. k_{nr}'s of **DCDPP** in both cluster and gas phase are strongly dependent on temperature, for instance, from 1.78×10^7 s^{-1} at 300 K to 9.04×10^5 s^{-1} (20 K), while the k_{nr} for the **DCPP** is almost independent on temperature,

5. DCPP has high fluorescence quantum yield which drops a little by aggregation at room temperature. Although **DCDPP** has very low fluorescence quantum yield which increases by aggregation, but remains always much smaller than that of **DCPP**.

The calculated temperature dependence of fluorescence quantum efficiency is depicted in Figure 2. It is seen that for the whole range of temperature, aggregation effect in **DCDPP** is found to enhance the fluorescence, about 150 times increase at 300 K and about six times increase at 20 K. We note that the experiment indicated that upon adding water in solution, the fluorescence quantum yield of **DCDPP** increases about 25 times when water fraction reaches 90% at room temperature.[6] Our results are in qualitative agreement with the experiment, given the fact that 90% water fraction does not mean ideal aggregate state as crystal used in our model. In fact, according to our previous argument, lowering temperature has a similar effect as aggregation for the nonradiative decay process. However, for **DCPP** with locked phenyl ring, there is hardly any appreciable aggregation effect, except some aggregation quenching at room temperature. This is again in good agreement with the experiment.[6]

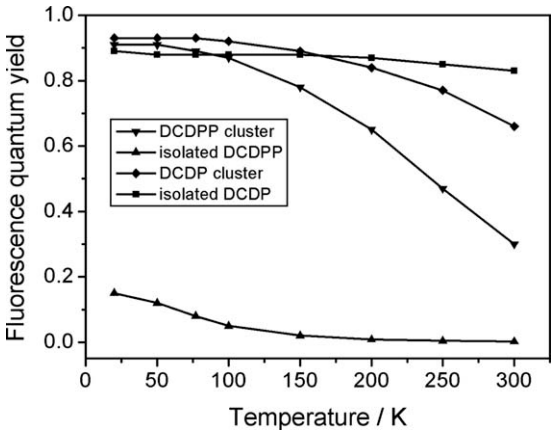

Figure 2. The calculated fluorescence quantum yields with temperature dependence for the **DCDPP** and **DCPP** (the values of the isolated DCDPP and DCPP molecules from the Ref. [14]).

Table 3. Selected bond lengths (Å), angles and torsion angles (°) of the S_0 and S_1 for the **DCDPP** molecule-in-cluster.

	DCDPP in cluster			Isolated **DCDPP**[a]			
	S_0	S_1	$\Delta(S_0–S_1)$	S_0	S_1	$\Delta(S_0–S_1)$	Crystal[b]
$C_1—C_2—C_3—C_4$	46.9	37. 7	9.2	36.0	20.0	16.0	51.60
$C_2—C_1—C_5—C_6$	44.7	40.5	4.2	36.0	20.0	16.0	44.15
$C_1—C_2—C_3$	123.0	122.6	0.4	125.2	123.0	2.2	
$C_1—C_2$	1.44	1.43	0.01	1.44	1.47	−0.03	
$C_2—C_3$	1.48	1.47	0.01	1.49	1.45	0.04	
$C_{11}—C_{12}$	1.41	1.46	−0.05	1.42	1.47	−0.05	
$C_2—N_9$	1.33	1.35	−0.02	1.34	1.34	0.0	
$N_9—C_{11}$	1.34	1.32	0.02	1.33	1.32	0.01	
$C_{11}—C_{13}$	1.44	1.43	0.01	1.44	1.43	0.01	

[a] Ref. [14]. [b] Ref. [6].

To reveal the underlying mechanism, we take a look at the molecular geometry and the excited state vibronic couplings. The optimized geometrical parameters for the ground state (S_0) and the first excited state (S_1) of the **DCDPP** and **DCPP** cluster with QM/MM method are summarized in Tables 3 and 4, respectively. We also predicted their energies in Supporting Information Table S1 and harmonic vibrational frequencies of the S_0 and S_1 for **DCDPP** and **DCPP** molecule in cluster in Supporting Information Tables S2–S6. In Table 3, the values of the most relevant structural parameters for the S_0 of DCDPP in the solid state are nearly the same with those in the gas phase except the two dihedral angels ($C_1—C_2—C_3—C_4$ and $C_2—C_1—C_5—C_6$), which show the rotations of the phenyl rings were influenced by aggregation. We found the changes of the two dihedral angles of DCDPP from the S_1 to S_0 are 9.2° and 4.2° for the cluster, whereas 16.0° and 16.0° for the isolated molecule.[14] This indicates that the structure for the excited process is more rigid in the solid state than that in the gas phase, namely, the rotations of the phenyl rings for the excited state are hindered in the solid state. From the Table 4, it can be seen that all the corresponding molecular parameters are

Table 4. Selected bond lengths (Å), angles and torsion angles (°) of the S_0 and S_1 for the **DCPP** molecule-in-cluster

	DCPP in cluster			Isolated **DCPP**[a]		
	S_0	S_1	$\Delta(S_0\text{-}S_1)$	S_0	S_1	$\Delta(S_0\text{-}S_1)$
$C_1—C_2—C_3—C_4$	−0.7	−0.9	0.2	0.0	0.0	0.0
$C_2—C_1—C_5—C_6$	0.5	1.0	−0.5	0.0	0.0	0.0
$C_1—C_2—C_3$	120.5	119.8	0.6	120.3	119.6	0.7
$C_1—C_2$	1.43	1.38	0.05	1.43	1.39	0.04
$C_2—C_3$	1.45	1.46	−0.01	1.46	1.40	−0.01
$C_{11}—C_{12}$	1.42	1.41	0.01	1.43	1.41	0.02
$C_4—C_6$	1.47	1.43	0.04	1.47	1.43	0.04
$C_2—N_9$	1.34	1.37	−0.03	1.34	1.37	−0.03
$N_9—C_{11}$	1.33	1.35	−0.02	1.33	1.35	−0.02
$C_{11}—C_{13}$	1.44	1.43	0.01	1.44	1.44	0.0

[a] Ref. [14].

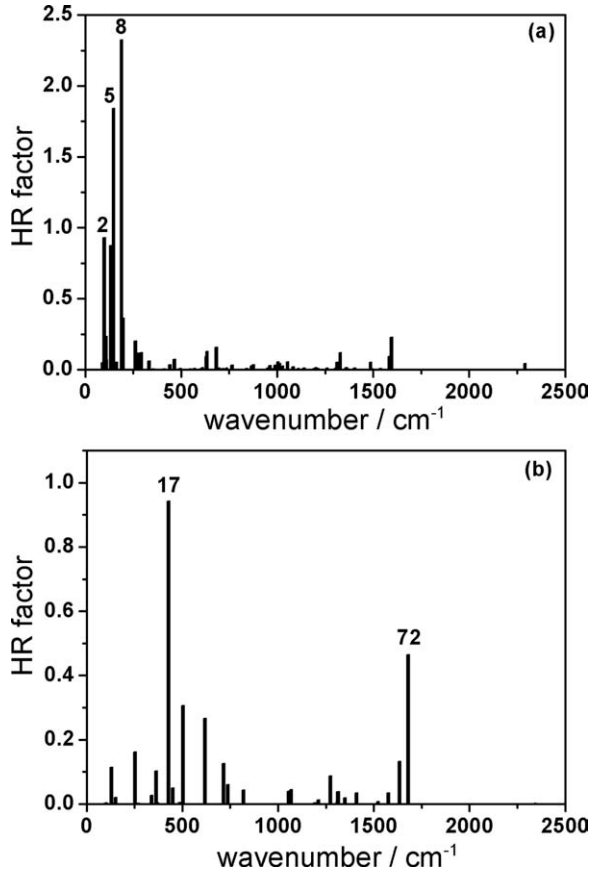

Figure 3. The calculated HR factors versus the normal mode wave numbers for the **DCDPP** cluster (a) and the **DCPP** cluster (b).

almost the same. From the comparison of the geometries for the **DCDPP** and **DCPP** cluster, it is clear that the restriction of intramolecular rotations is the main cause for the novel AIE phenomenon.[3–6] Moreover, the QM/MM predicted dihedral angles (46.9° and 44.7°) of the **DCDPP** cluster are in better agreement with the results of the X-ray diffraction (51.60° and 44.15°),[6] which also indicates the QM/MM approach is well fit for the organic molecule systems.

Huang–Rhys (HR) factor $HR_j = \left(\omega_j D_j^2\right)/2\hbar$ characterizes the modification of vibrational quanta when going from one electronic state to another for the *j*th vibrational mode, which are important for determining the IC rate.[12,13] For **DCDPP** in cluster, HR factors are depicted in Figure 3a and some selected HR factors *versus* corresponding normal modes in Supporting Information Table S6. It is seen that (i) three modes with large HR factors (>1.0) all appear at the low frequency region (<200 cm^{-1}); (ii) the HR factors of the **DCDPP** in cluster is much smaller than those of the isolated **DCDPP** for the same modes, the detail of the HR factors for the isolated **DCDPP** are reported in Ref. [14]. For comparison, we also presented the HR factors of the first excited state for the **DCPP** cluster in Figure 3b and some selected HR factors *versus* corresponding normal modes in Supporting Information Table S7. It can be seen that (i) the HR factors are all very small, even the largest for the mode 17 is not more than 1.0; (ii) the HR factors do not change much from the gas phase (see Ref. [14]) to the solid state. For the sake of clarity, the normal modes of the three lower vibrational frequencies for the **DCDPP** cluster are shown in Supporting Information Figure S3 and are assigned to the phenyl rings twisting which suggest the low-frequency motions of the phenyl rings are hindered in the solid state. Therefore, the energy dissipation via nonradiative channel can be blocked by aggregation and the radiative decay became dominant, namely, when k_{nr} is mainly contributed by the modes of the lower frequency motions. The normal harmonic vibrational modes of the 17 and 72 for the **DCPP** in cluster are depicted in Supporting Information Figure S4, which showed that the mode for 72 belong to the C=C stretching. As in many conjugated molecules, the C=C stretching dominates the vibronic coupling for excited state decay process and does not present the exotic AIE phenomena. Only when the low-frequency motions are coupled strongly with the excited state, can AIE occurs, as speculated earlier.[12,13] These can be further elucidated by the reorganization energies of the first excited state for the **DCDPP** and **DCPP** cluster, see Supporting Information Figure S5. It is found that (i) the contribution of the three lower frequency modes (<200 cm^{-1}) contribute about 27.4% for the **DCDPP** in cluster; (ii) the largest contribution for the reorganization energy of the **DCPP** is the high frequency with the C=C stretching, which is insensitive to aggregation. These results further confirm that the large contribution of the low-frequency modes to the k_{nr} is the main cause for the novel AIE phenomenon.

Conclusions

In summary, using a QM/MM approach, we have investigated the aggregation effects on the excited state decays, both via radiative and nonradiative routes, for the **DCDPP** and **DCPP** molecule-in-cluster. The rotations of the phenyl rings in **DCDPP** are found to play important role in dissipating excited state energy and are found to be hindered in the aggregate. The fluorescence quantum efficiency is increased 150 times upon aggregation at room temperature, exhibiting prominent AIE phenomena. The experimental value is about 25 times increase. But for the phenyl ring locked molecule **DCPP**, the major energy dissipation route is found to be C=C stretching, as in most conjugated system, which does not exhibit appreciable aggregation effects, which is in good agreement with the experiment. The normal aggregation quenching effects due to intermolecular charge or energy transfer or Davydov splittings are not considered in this study. In all the cases, the radiative decay rates are found to be almost independent on either temperature or aggregation. The primary origin of the exotic AIE phenomena is found due to the nonradiative decay effects. That is, aggregation can confine the molecules into a more rigid environment, which can block efficient nonradiative decay processes in molecules with low-frequency vibrational modes. Upon photoexcitations, the low-frequency motions such as phenyl ring twisting motions become mixed each other, which largely contribute to the FC overlaps for different normal modes between two electronic state potential energy surfaces. Such mixing termed as Duschinsky rotation becomes

much less effective for high-frequency motions. Last, certainly not the least, in the present work, we did not consider the excitonic effect including the Davydov splitting, which deserves further investigation, which probably is the reason for our overestimation of the aggregation effect.

Acknowledgments

The authors thank Professor Zexing Cao, Dr. Dongqi Wang for the many helps about the Chemshell package. Valuable discussions with Prof. Eli Pollak and Prof. Jiushu Shao are acknowledged.

Keywords: nonadiabatic dynamics · excited state decay · aggregation induced emission

How to cite this article: Q. Wu, C. Deng, Q. Peng, Y. Niu, Z. Shuai, *J. Comput. Chem.* **2012,** *00,* 000–000. DOI: 10.1002/jcc.23019

Additional Supporting Information may be found in the online version of this article.

[1] (a) J. G. C. Veinot, T. J. Marks, *Acc. Chem. Res.* **2005**, *38,* 632; (b) U. Mitschke, P. J. Bäuerle, *J. Mater. Chem.* **2000**, *10,* 1471; (c) C.-T. Chen, *Chem. Mater.* **2004**, *16,* 4389.

[2] (a) D. Sainova, T. Miteva, G. Nothofer, U. Scherf, I. Glowacki, J. Ulanski, H. Fujikawa, D. Neher, *Appl. Phys. Lett.* **2000**, *76,* 1810; (b) S. Hecht, J. M. Frechet, *Angew. Chem. Int. Ed. Engl.* **2001**, *40,* 74.

[3] J. Luo, Z. Xie, J. W. Y. Lam, L. Cheng, H. Chen, C. Qiu, H. S. Kwok, X. Zhan, Y. Liu, D. Zhu, B. Tang, *Chem. Commun.* **2001**, 1740.

[4] B. Tang, X. Zhan, G. Yu, P. Lee, Y. Liu, D. Zhu, *J. Mater. Chem.* **2001**, *11,* 2974.

[5] G. Yu, S. Yin, Y. Liu, J. Chen, X. Xu, X. Sun, D. Ma, X. Zhan, Q. Peng, Z. Shuai, B. Z. Tang, D. Zhu, W. Fang, Y. Luo, *J. Am. Chem. Soc.* **2005**, *127,* 6335.

[6] A. Qin, J. W. Y. Lam, F. Mahtab, C. K. W. Jim, L. Tang, J. Sun, H. Y. Sung, I. D. Williams, B. Z. Tang, *Appl. Phys. Lett.* **2009**, *94,* 253308.

[7] Z. Li, Y. Dong, B. Mi, Y. Tang, M. Häussler, H. Tong, Y. Dong, J. W. Y. Lam, Y. Ren, H. H. Y. Sung, K. S. Wong, P. Gao, I. D. Williams, H. S. Kwok, B. Z. Tang, *J. Phys. Chem. B* **2005**, *109,* 10061.

[8] B.-K. An, S.-K. Kwon, S.-D. Jung; S. Y. Park, *J. Am. Chem. Soc.* **2002**, *124,* 14410.

[9] Y. Liu, X. Tao, F. Wang, J. Shi, J. Sun, W. Yu, Y. Ren, D. Zou, M. Jiang, *J. Phys. Chem. C* **2007**, *111,* 6544.

[10] Y. Sonoda, S. Tsuzuki, M. Goto, N. Tohnai, M. Yoshida, *J. Phys. Chem. A* **2010**, *114,* 172.

[11] R. Hu, E. Lager, A. Aguilar-Aguilar, J. Liu, J. W. Y. Lam, H. H. Y. Sung, I. D. Williams, Y. Zhong, K. S. Wong, E. Peña-Cabrera, B. Z. Tang, *J. Phys. Chem. C* **2009**, *113,* 15845.

[12] S. Yin, Q. Peng, Z. Shuai, W. Fang, Y. Wang, Y. Luo, *Phys. Rev. B* **2006**, *73,* 205409.

[13] Q. Peng, Y. Yi, Z. Shuai, J. Shao, *J. Am. Chem. Soc.* **2007**, *129,* 9333.

[14] C. Deng, Y. Niu, Q. Peng, A. Qin, Z. Shuai, B. Z. Tang, *J. Chem. Phys.* **2011**, *135,* 014304.

[15] M. C. Li, M. Hayashi, S. H. Lin, *J. Phys. Chem. A* **2011**, *115,* 14531.

[16] (a) A. Frad, F. Lahmani, A. Tramer, C. Tric, *J. Chem. Phys.* **1974**, *60,* 4419; (b) S. Hillenbrand, L. Zhu, P. Johnson, *J. Chem. Phys.* **1990**, *92,* 870; (c) M. Tsubouchi, B. J. Whitaker, T. Suzuki, *J. Phys. Chem. A* **2004**, *108,* 6823; (d) G. Stock, W. Domcke, *J. Phys. Chem.* **1993**, *97,* 12466; (e) P. S. Christopher, M. Shapiro, P. Brumer, *J. Chem. Phys.* **2006**, *124,* 184107; (f) P. S. Christopher, M. Shapiro, P. Brumer, *J. Chem. Phys.* **2006**, *125,* 124310; (g) I. Burghardt, K. Giri, G. A. Worth, *J. Chem. Phys.* **2008**, *129,* 174104; (h) R. Islampour, M. Miralinaghi, *J. Phys. Chem. A* **2009**, *113,* 2340.

[17] (a) F. Bernardi, S. De, M. Olivucci, M. A. Robb, *J. Am. Chem. Soc.* **1990**, *112,* 1737; (b) M. Reguero, M. Olivucci, F. Bernardi, M. A. Robb, *J. Am. Chem. Soc.* **1994**, *116,* 2103; (c) M. J. Bearpark, F. Bernardi, S. Clifford, M. Olivucci, M. A. Robb, B. R. Smith, T. Vreven, *J. Am. Chem. Soc.* **1996**, *118,* 169; (d) V. Vallet, Z. Lan, S. Mahapatra, A. L. Sobolewski, W. Domcke, *J. Chem. Phys.* **2005**, *123,* 144307; (e) B. G. Levine, T. J. Martinez, *Annu. Rev. Phys. Chem.* **2007**, *58,* 613; (f) W. R. Duncan, O. V. Prezhdo, *Annu. Rev. Phys. Chem.* **2007**, *58,* 143; (g) Z. Lan, E. Fabiano, W. Thiel, *J. Phys. Chem. B* **2009**, *113,* 3548.

[18] (a) H.-D. Meyer, W. H. Miller, *J. Chem. Phys.* **1980**, *72,* 2272; (b) P. Salek, O. Vahtras, T. Helgaker, H. Ågren, *J. Chem. Phys.* **2002**, *117,* 9630; (c) J. E. Subotnik, *J. Chem. Phys.* **2010**, *132,* 134112.

[19] (a) J. C. Tully, *J. Chem. Phys.* **1990**, *93,* 1061; (b) S. Hammes-Schiffer, J. C. Tully, *J. Chem. Phys.* **1994**, *101,* 4657; (c) O. V. Prezhdo, *J. Chem. Phys.* **1999**, *111,* 8366; (d) J. R. Schmidt, P. V. Parandekar, J. C. Tully, *J. Chem. Phys.* **2008**, *129,* 044104.

[20] H. D. Meyer, U. Manthe, L. S. Cederbaum, *Chem. Phys. Lett.* **1990**, *165,* 73.

[21] (a) U. Manthe, H. D. Meyer, L. S. Cederbaum, *J. Chem. Phys.* **1992**, *97,* 3199; (b) G. A. Worth, H.-D. Meyer, L. S. Cederbaum, *J. Chem. Phys.* **1998**, *109,* 3518; (c) A. Raab, G. A. Worth, H.-D. Meyer, L. S. Cederbaum, *J. Chem. Phys.* **1999**, *110,* 936; (d) M. H. Beck, A. Jäckle, G. A. Worth, H.-D. Meyer, *Phys. Rep.* **2000**, *324,* 1; (e) G. A. Worth, H.-D. Meyer, H. Köppel, L. S. Cederbaum, I. Burghardt, *Int. Rev. Phys. Chem.* **2008**, *27,* 569.

[22] (a) M. Hayashi, A. M. Mebel, K. K. Liang, S. H. Lin, *J. Chem. Phys.* **1998**, *108,* 2044; (b) A. M. Mebel, M. Hayashi, K. K. Liang, S. H. Lin, *J. Phys. Chem. A* **1999**, *103,* 10674.

[23] (a) G. W. Robinson, R. P. Frosch, *J. Chem. Phys.* **1962**, *37,* 1962; (b)W. Robinson, R. P. Frosch, *J. Chem. Phys.* **1963**, *38,* 1187.

[24] (a) S. H. Lin, *J. Chem. Phys.* **1966**, *44,* 3759; (b) S. H. Lin, R. Bersohn, *J. Chem. Phys.* **1968**, *48,* 2732; (c) S. H. Lin, *J. Chem. Phys.* **1973**, *58,* 5760; (d) M. Bixon, J. Jortner, *J. Chem. Phys.* **1968**, *48,* 715; (e) M. Bixon, J. Jortner, *J. Chem. Phys.* **1969**, *50,* 4061; (f) A. Nitzan, J. Jortner, *J. Chem. Phys.* **1971**, *55,* 1355; (g) W. Siebrand, *J. Chem. Phys.* **1971**, *54,* 363 (h) S. Fischer, *Chem. Phys. Lett.* **1971**, *11,* 577; (i) D. F. Heller, K. F. Freed, W. M. Gelbart, *J. Chem. Phys.* **1972**, *56,* 2309.

[25] Y. Niu, Q. Peng, C. Deng, X. Gao, Z. Shuai, *J. Phys. Chem. A* **2010**, *114,* 7817.

[26] (a) Q. Peng, Y. Yi, Z. Shuai, J. Shao, *J. Chem. Phys.* **2007**, *126,* 114302; (b) C. W. Müller, J. J. Newby, C.-P. Liu, C. P. Rodrigo, T. S. Zwier, *Phys. Chem. Chem. Phys.* **2010**, *12,* 2331.

[27] Y. Niu, Q. Peng, Z. Shuai, *Sci. China Ser. B Chem.* **2008**, *51,* 1153.

[28] J. R. Reimers, *J. Chem. Phys.* **2001**, *115,* 9103.

[29] (a) S. A. French, A. A. Sokol, S. T. Bromley, C. R. A. Catlow, S. C. Rogers, F. King, P. Sherwood, *Angew. Chem. Int. Ed. Engl.* **2001**, *40,* 4437; (b) O. Acevedo, W. L. Jorgensen, *J. Am. Chem. Soc.* **2006**, *128,* 6141; (c) J. To, P. Sherwood, A. A. Sokol, I. J. Bush, C. R. A. Catlow, H. J. J. van Dam, S. A. French, M. F. Guest, *J. Mater. Chem.* **2006**, *16,* 1919; (d) S. Tsushima, U. Wahlgren, I. Grenthe, *J. Phys. Chem. A* **2006**, *110,* 9175; (e) H. M. Senn, W. Thiel, *Curr. Opin. Chem. Biol.* **2007**, *11,* 182; (f) H. Lin, D. G. Truhlar, *Theor. Chem. Acc.* **2007**, *117,* 185; (g) J. Torras, S. Bromley, O. Bertran, F. Illas, *Chem. Phys. Lett.* **2008**, *457,* 154; (h) H. M. Senn, W. Thiel, *Angew. Chem. Int. Ed. Engl.* **2009**, *48,* 1198; (i) M. Parac, M. Doerr, C. M. Marian, W. Thiel, *J. Comput. Chem.* **2010**, *31,* 90.

[30] P. Sherwood, A. H. de Vries, M. F. Guest, G. Schreckenbach, C. R. A. Catlow, S. A. French, A. A. Sokol, S. T. Bromley, W. Thiel, A. J. Turner, S. Billeter, F. Terstegen, S. Thiel, J. Kendrick, S. C. Rogers, J. Casci, M. Watson, F. King, E. Karlsen, M. Sjovoll, A. Fahmi, A. Schafer and C. Lennartz, *J. Mol. Struct. (Theochem)* **2003**, *632,* 1.

[31] S. R. Billeter, A. J. Turner, W. Thiel, *Phys. Chem. Chem. Phys.* **2000**, *2,* 2177.

[32] (a) R. Ahlrichs, M. Bar, M. Haser, H. Horn, C. Kolmel, *Chem. Phys. Lett.* **1989**, *162,* 165; (b) P. Deglmann, F. Furche, *J. Chem. Phys.* **2002**, *117,* 9535; (c) P. Deglmann, F. Furche, R. Ahlrichs, *Chem. Phys. Lett.* **2002**, *362,* 511; (d) F. Furche, R. Ahlrichs, *J. Chem. Phys.* **2002**, *117,* 7433.

[33] W. Smith, T. R. Forester, *J. Mol. Graph.* **1996**, *14,* 136.

[34] J. Wang, R. M. Wolf, J. W. Caldwell, P. A. Kollamn, D. A. Case, *J. Comput. Chem.* **2004**, *25,* 1157.

[35] D. Bakowies, W. Thiel, *J. Phys. Chem.* **1996**, *100,* 10580.

[36] M. J. Frisch, G. W. Trucks, H. B. Schlegel, G. E. Scuseria, M. A. Robb, J. R. Cheeseman, G. Scalmani, V. Barone, B. Mennucci, G. A. Petersson, H. Nakatsuji, M. Caricato, X. Li, H. P. Hratchian, A. F. Izmaylov, J. Bloino, G.

Zheng, J. L. Sonnenberg, M. Hada, M. Ehara, K. Toyota, R. Fukuda, J. Hasegawa, M. Ishida, T. Nakajima, Y. Honda, O. Kitao, H. Nakai, T. Vreven, J. A. Montgomery, Jr., J. E. Peralta, F. Ogliaro, M. Bearpark, J. J. Heyd, E. Brothers, K. N. Kudin, V. N. Staroverov, R. Kobayashi, J. Normand, K. Raghavachari, A. Rendell, J. C. Burant, S. S. Iyengar, J. Tomasi, M. Cossi, N. Rega, J. M. Millam, M. Klene, J. E. Knox, J. B. Cross, V. Bakken, C. Adamo, J. Jaramillo, R. Gomperts, R. E. Stratmann, O. Yazyev, A. J. Austin, R. Cammi, C. Pomelli, J. W. Ochterski, R. L. Martin, K. Morokuma, V. G. Zakrzewski, G. A. Voth, P. Salvador, J. J. Dannenberg, S. Dapprich, A. D. Daniels, Ö. Farkas, J. B. Foresman, J. V. Ortiz, J. Cioslowski, and D. J. Fox, J. Gaussian, Inc., Wallingford CT, **2009**.

[37] F. Spano, *Acc. Chem. Res.* **2010**, *43,* 429.

Received: 7 February 2012
Revised: 9 April 2012
Accepted: 22 April 2012
Published online on